

ACI Foundation – Final Report **October 2023**

Structural nanomodified concrete: an investigation of critical properties

Principal Investigator: Dr. David J Corr
Clinical Professor and Director of Graduate Studies
Department of Civil & Environmental Engineering
Northwestern University
d-corr@northwestern.edu
Note: Dr. Corr has resigned from Northwestern University and can now be contacted at:
dcorr@ctlgroup.com

Co-Investigators: Dr. Surendra P Shah and Dr. Maria Konsta-Gdoutos
University of Texas at Arlington

Project Objectives

The objectives of this project were to investigate long term mechanical and durability characteristics of nanomodified concrete. With the incorporation of well dispersed CNT/CNF it is expected that properties such as creep, shrinkage and corrosion will be influenced. Specifically, at the conclusion of the project, we will have examined:

- **Creep behavior of CNT/CNF nanomodified concrete**
- **Shrinkage properties of CNT/CNF nanomodified concrete**
- **Corrosion potential of CNT/CNF nanomodified concrete**

Background and Significance

Nanotechnology in cementitious composites is one of the most promising new technologies available to the concrete industry [1-3]. Fiber-shaped nanomaterials such as carbon nanotubes (CNT) and carbon nanofibers (CNF) have shown particular promise in improving properties such as elastic modulus and flexural strength [4,5]. With the goal of bringing these materials to market, this study aims to evaluate other critical properties like corrosion, creep and shrinkage of nanomodified composites. The approach presented here uses very small additions of CNF for nanomodification. For the rest of this document CNF are discussed; however prior studies have shown similar properties between CNT and CNF, and it is expected that the results of this study can also guide the use of CNT [6].

Experimental Program and Results: General Information

Initially begun pre-pandemic, the proposed study experienced several significant and unexpected setbacks, including a complete shutdown of our laboratory in 2020 due to COVID

which affected experiments in progress, and subsequent equipment failures at NU facilities that affected our ability to restart large-scale experimental programs. As these issues were being resolved, students working on this project continued to progress towards degrees, and ultimately graduated after working on topics that were related to the proposed work but more feasible to complete given the altered work environment during COVID. These studies yielded significant contributions to understanding of nanomaterial dispersion and creep measurement - this final report summarizes the outcomes and contributions of these efforts; further information about the prior experiments on uniaxial creep, shrinkage and corrosion are available in the interim report on this project.

Dispersion Particle Size Characterization

Adequate dispersion of CNF in an aqueous solution is critical to performance of finished concrete materials [2], [7]. Figure 1(a) shows a Scanning Electron Microscopy (SEM) image of undispersed CNF in aqueous solutions, with clear agglomeration of the CNF. Figure 1(b) shows another SEM image of a well dispersed CNF aqueous solution, where individual fibers are dispersed from one another. A method using ultrasonication and polycarboxylate superplasticizer (SP) is used to disperse CNF [8], [9]. Using this method, very small quantities of CNF (on the order of 0.1% by weight of cement) show a noticeable improvement in desirable mechanical properties such as elastic modulus, cracking resistance, and flexural strength. Similar dispersion methods have been in use in laboratory studies on CNT and CNF for some time, but there is not an understanding of how the mechanical energy used affects the size distribution of the nanomaterials in the dispersion.

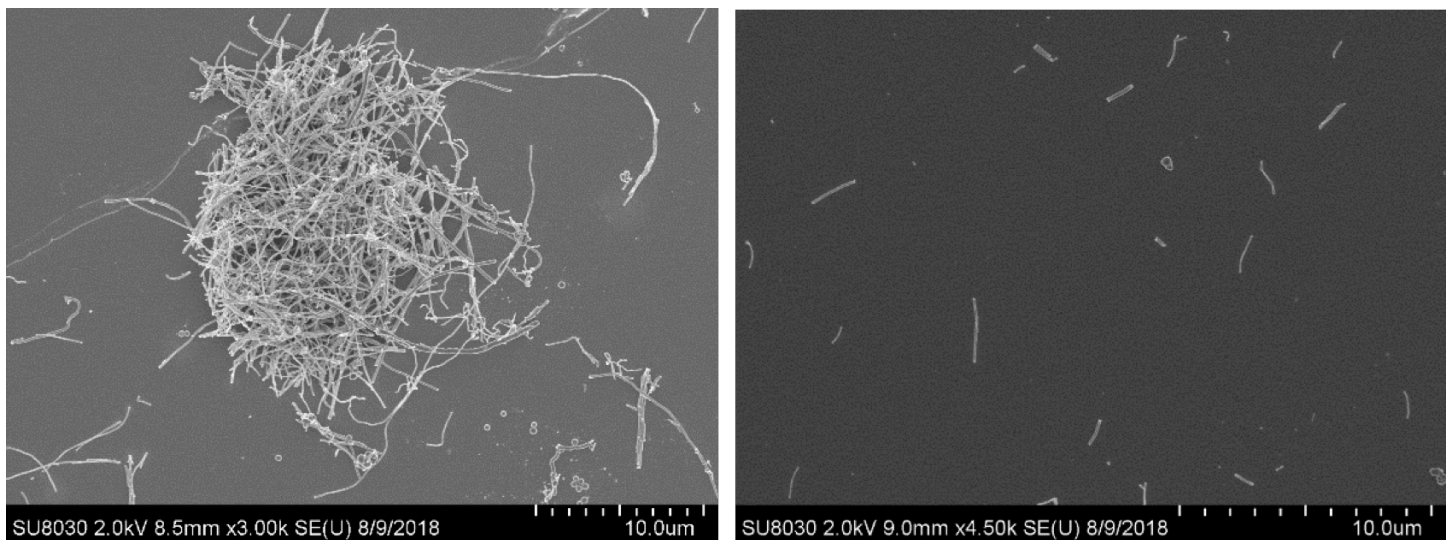


Figure 1: Difference between (a) Undispersed and (b) Dispersed CNF (using the DTC method described below) in aqueous solutions

Figure 1(b) is not trivial to acquire, as imaging dispersed aqueous nanomaterials often results in numerous overlapping layers, confounding efforts to characterize fiber features. To examine individual fiber dispersion characteristics, methods such as Ultraviolet-Visible Spectroscopy

(UV-Vis) are used in conjunction with Scanning Electron Microscopy (SEM) and Atomic Force Microscopy (AFM) techniques [10]. A well dispersed solution is obtained when the UV-Vis peak absorption shows a plateau with increase in energy. Fig 2.(a) is a representation of a typical UV-Visible Spectroscopy absorption spectrum and 2(b) shows the peak absorption which plateaus with ultrasonication provided to the suspension.

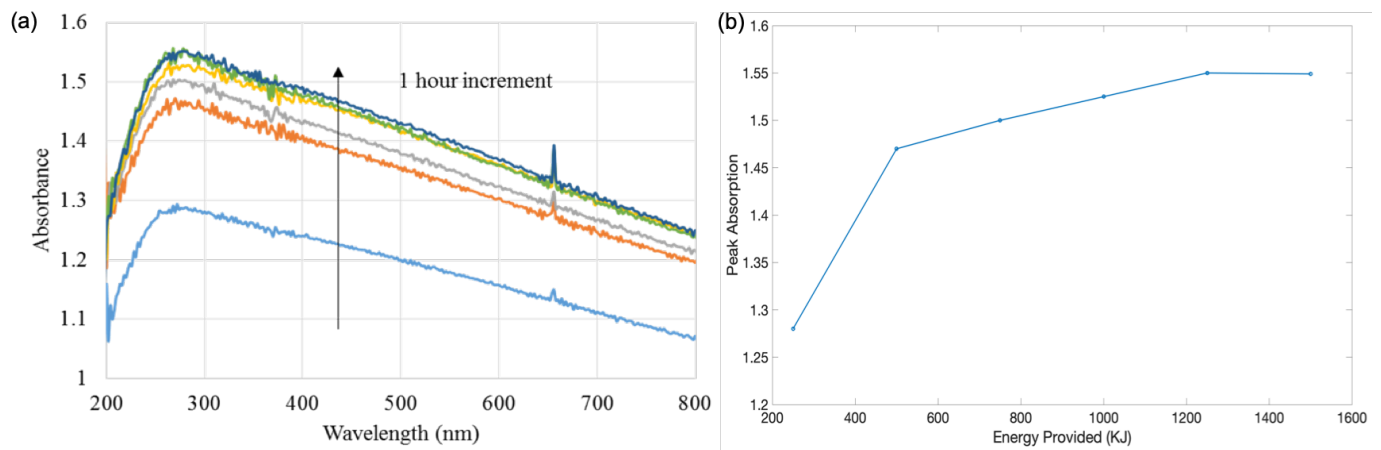


Figure 2: (a) Ultraviolet Visible Spectroscopy (b) Peak absorption versus energy provided (kJ) to disperse aqueous CNF suspensions

In order to visualize CNF using SEM and AFM and to characterize the geometry and shape of fibers, drop test characterization (DTC) is a technique developed to investigate monolayers of dispersed CNF on a silicon substrate – this allows imaging and measurement of size distribution of fibers. Further details of DTC are discussed in [11] and [12] but are presented in a condensed form here. DTC begins with a silicon wafer prepared with a standard cleaning procedure, using acetone, isopropyl alcohol (IPA) and deionized (DI) water, bath sonicated for 5 minutes in each solvent and then dried using a nitrogen gun. Following the cleaning, the substrates are coated with 3-(Aminopropyl) triethoxysilane (APTES) solution, forming a mono layer of APTES nodes on the substrate. This process forms a substrate with functional amine groups which will attract dispersed CNF particles when a drop of the suspension is introduced. The excess suspension is then removed by rinsing with DI water, after which the specimen is prepared for imaging and characterization of the CNF monolayer.

Figure 3 shows SEM images of CNF monolayers produced by DTC (3(a) through 3(d) at four increasing dispersion durations), coupled with the size distribution histograms that can be developed through image processing (3(e) through 3(h)) of the SEM images. Notable results seen here: first, the average lengths of the CNT (1-2 μ m) are considerably shorter than the original material, with CNT lengths in 100s of μ m as reported by the manufacturer. Second, the mean fiber length decreases by nearly fifty percent during the energy application of sonication. This rate decreases slowly with the increase of energy, which is in accordance with trends in other dispersion characterization techniques such as UV-Vis as shown in Fig. 2(b).

Further discussion of the method and findings of dispersion characterization, and what this study reveals about nanomodified cementitious composite performance is available in [11] and [12].

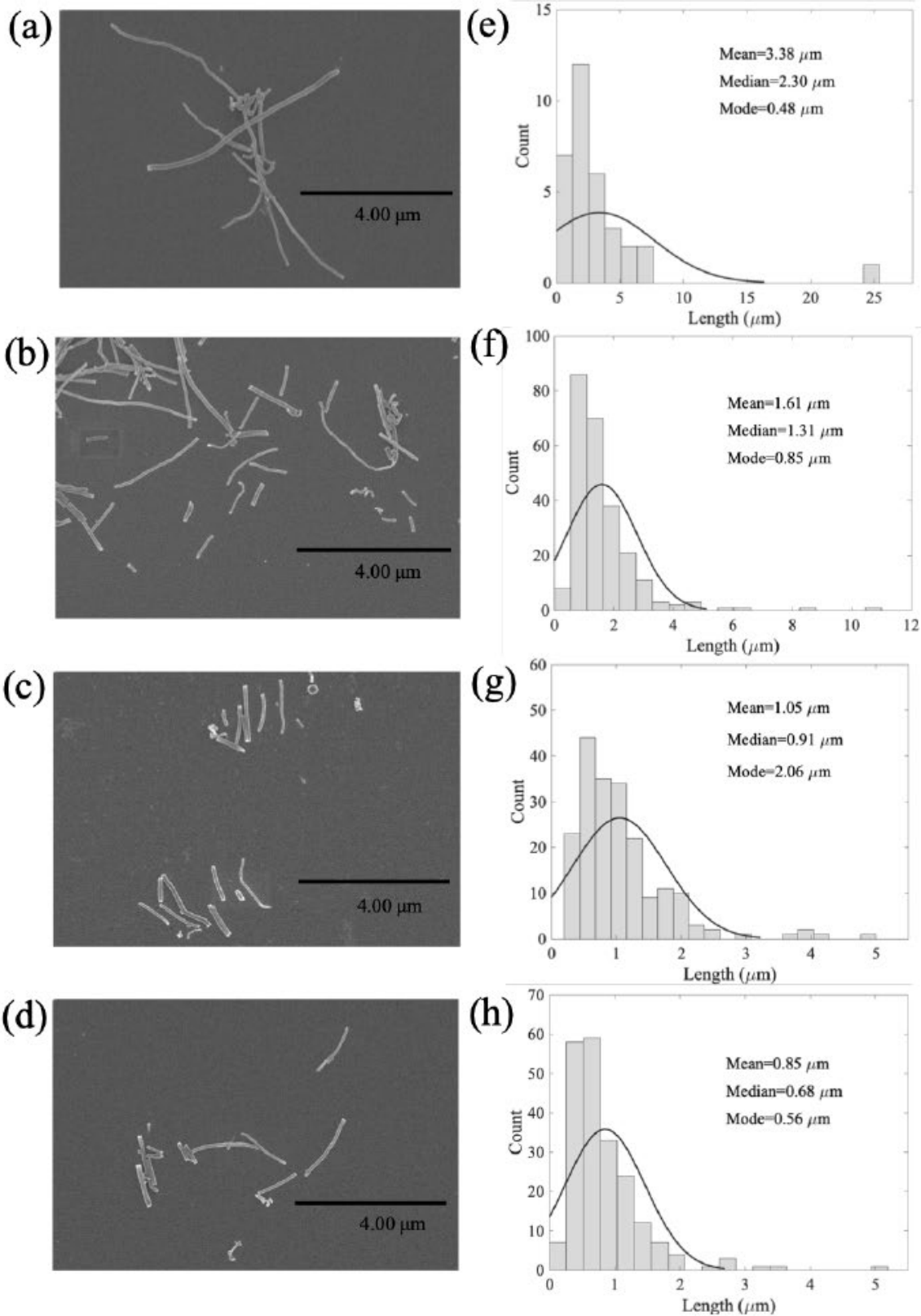


Figure 3: SEM images (a-d) and statistical information on size distribution of dispersed CNF (e-h) at 1 hr (figs a/e), 2 hr (figs b/f), 4 hr (figs c/g) and 8 hr (figs d/h) of dispersion

Contact Creep Characterization

Creep behavior is a crucial property of concrete since structural elements that deform progressively due to a constant applied load can cause serviceability issues and, if excessive, safety concerns. Concrete's creep behavior comes mainly from logarithmic creep kinetics of the cement paste, since aggregates are stiffer and not typically prone to creep deformation. The cementitious matrix properties, loading conditions, and environmental conditions are the dictating factors that control concrete creep behavior. Since concrete's elastic modulus increases by 30 - 50 % with the addition of 0.1 wt. % CNF, the expected change is a decrease in creep compliance.

While the conventional test used to measure creep in concrete is the long-term uniaxial creep test, another technique to study the creep behavior is to measure the contact creep modulus from statistical nano- or micro- indentation tests performed on the cement paste. The measured creep modulus of the uniaxially loaded specimen can be approximated by homogenization through the Mori-Tanaka method and measurements of contact creep modulus. Compared to the uniaxial loaded test, measurement of contact creep can be performed in a few hours for each sample. In this study, the creep in CNF-modified cement composites are evaluated from nanoindentation and microindentation measurements that can predict the uniaxial creep behavior. Details of this method and the measurement of creep behavior from indentation results are detailed in [13], and are discussed in a condensed form here.

Following sample preparation, nanoindentation is performed using a Hysitron Triboindenter, which is depicted in Figure 4. The nanoindentations are performed in a 10 by 10 grid with a spacing of 10 μm . A trapezoidal control load procedure is applied onto the specimen surface (Figure 4a). The procedure contains three phases: (1) 0.25 mN/s constant rate loading phase, (2) 10 second holding phase at $P_{max} = 2500 \mu N$ (2.5 mN), and (3) 0.25 mN/s constant rate unloading phase. Figure 4b shows an atomic force microscopy (AFM) – tapping mode surface map of a series of nanoindentations marks. Figure 4c shows a representative indentation force $P(t)$ versus indentation depth $h(t)$ of a nanoindentation for the loading, holding, and unloading phases of a sample. Figure 4d shows the result of the contact creep function calculated from the data obtained at the holding phase of the trapezoidal procedure, which is the region marked with a yellow ellipsoid in Figure 4c. The key parameter in this image is C_i , the indentation contact creep modulus.

These nanoindentation tests are completed on cement paste samples with and without CNF, and with w/c varying between 0.3 and 0.5. Nanoindentation has the potential to sample large numbers of points on a material surface, yielding statistics on the properties of the material and the phases it contains. A gaussian deconvolution scheme is used to calculate the effect of four phases in each sample (porous regions, LD C-S-H, HD C-S-H, and intermixed CH/C-S-H regions), which is discussed in [13]. The resulting measurements of elastic modulus, hardness, and contact creep modulus for these four phases is summarized in Table 1. The nanoindentation data is also depicted as histograms in Figure 5, where previously reported 30-50% differences

with CNT addition are seen in elastic modulus, with even larger impacts on hardness and contact creep modulus. It is important to note that the large increase in contact creep modulus seen in Figure 5 incorporates two effects: the underlying increased mechanical hardness increase due to CNF addition, as well as changes to C-S-H, presumably chemical or structural in nature (which can also alter hardness) due to seeding or other effects of CNF. The first effect (CNF hardness's impact on contact creep modulus) can be removed by plotting contact creep modulus against hardness as shown in Figure 6. Here it can be seen that there is an approximately linear relationship between hardness and contact creep, with the slope of that relationship being increased in the presence of CNF. This result has important implications in the estimation of bulk creep behavior via indentation – a much simpler and faster method to run than a long-term uniaxial creep test. Measurements of hardness from methods with less resolution than nanoindentation (such as microindentation) can have the potential to predict uniaxial behavior due to this linear relationship between hardness and creep modulus.

In-depth discussion of the method and findings of contact creep measurement and modeling, and how it can be used as a predictor for uniaxial creep behavior is available in [13] and [14].

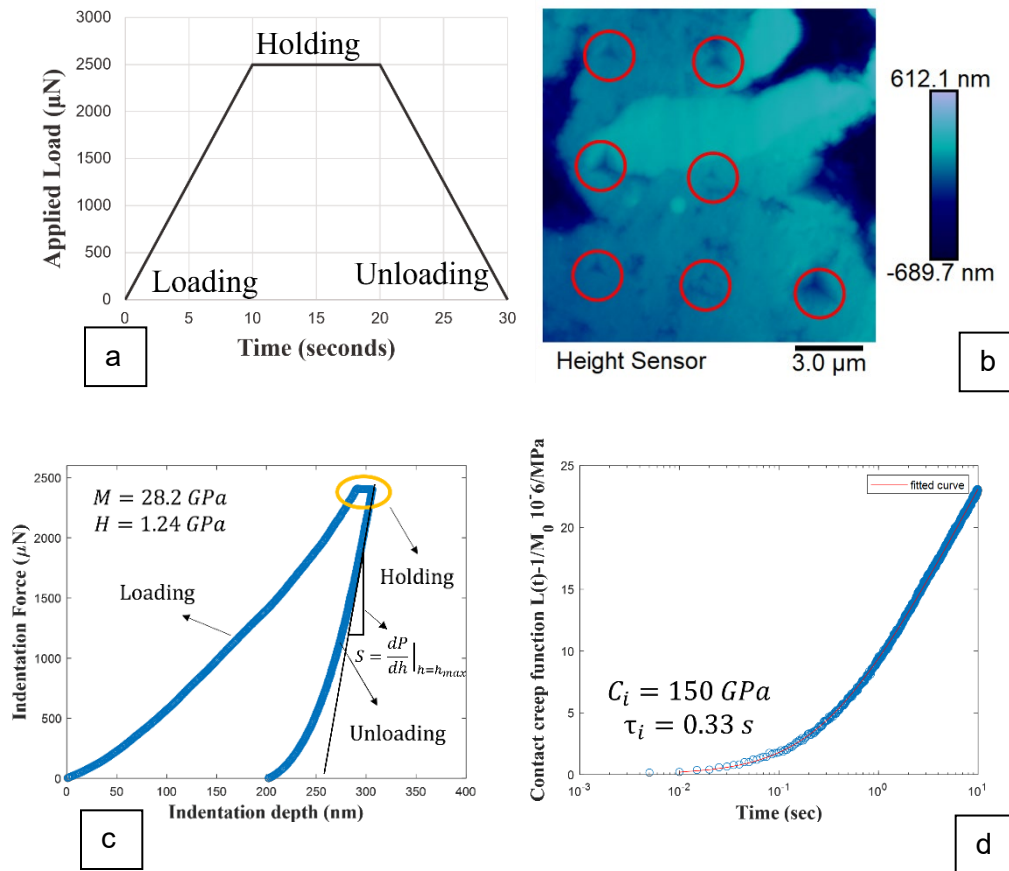


Figure 4: a. Trapezoidal load control protocol, b. AFM - tapping mode surface map of nanoindentations, c. indentation force (P) versus indentation depth (h), and d. contact creep function obtained from holding phase

Table 1: Elastic modulus, hardness, and contact creep modulus calculated from deconvolution of nanoindentation data

Sample	Surface fraction [%]	Elastic Modulus [GPa]	Hardness [GPa]	Contact Creep Modulus [GPa]
w/c = 0.3				
- Porosity	6	5.7 ± 1.0	0.08 ± 0.04	100 ± 20
- LD C-S-H	75	18.5 ± 3.8	0.59 ± 0.26	163 ± 42
- HD C-S-H	7	29.8 ± 1.6	1.36 ± 0.23	291 ± 31
- CH/C-S-H	12	41.8 ± 4.9	2.22 ± 0.39	559 ± 225
w/c = 0.3 0.1wt.% CNFs				
- Porosity	6	10.0 ± 3.8	0.32 ± 0.12	128 ± 39
- LD C-S-H	47	20.1 ± 3.5	0.86 ± 0.26	324 ± 63
- HD C-S-H	31	28.2 ± 3.3	1.36 ± 0.23	429 ± 43
- CH/C-S-H	16	40.9 ± 9.4	2.61 ± 0.39	564 ± 21
w/c = 0.4 0.1wt.% CNFs				
- Porosity	6	10.1 ± 1.0	0.29 ± 0.08	201 ± 24
- LD C-S-H	38	18.4 ± 2.4	0.66 ± 0.28	408 ± 37
- HD C-S-H	33	26.6 ± 1.0	1.34 ± 0.20	524 ± 47
- CH/C-S-H	23	37.7 ± 1.9	2.54 ± 0.41	769 ± 75
w/c = 0.5 0.1wt.% CNFs				
- Porosity	6	4.9 ± 1.6	0.07 ± 0.03	134 ± 21
- LD C-S-H	65	18.0 ± 4.8	0.62 ± 0.22	478 ± 66
- HD C-S-H	23	34.3 ± 3.7	0.98 ± 0.14	565 ± 20
- CH/C-S-H	6	46.1 ± 5.6	2.45 ± 0.42	663 ± 78

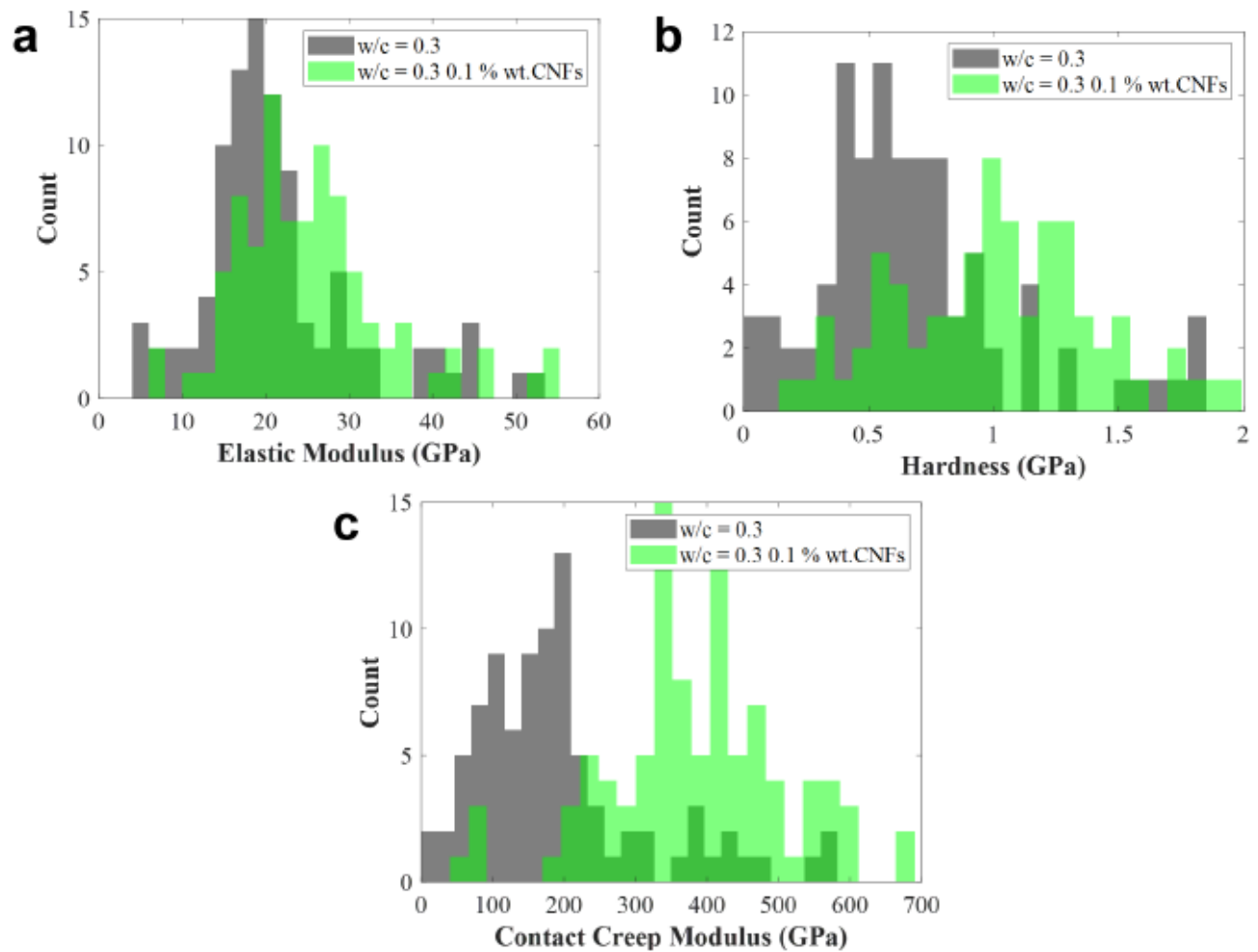


Figure 5: Histograms of elastic modulus, hardness, and contact creep modulus for 0.3 w/c paste, both with and without CNF. CNF addition produces higher values in all metrics, with the effect most pronounced for contact creep modulus.

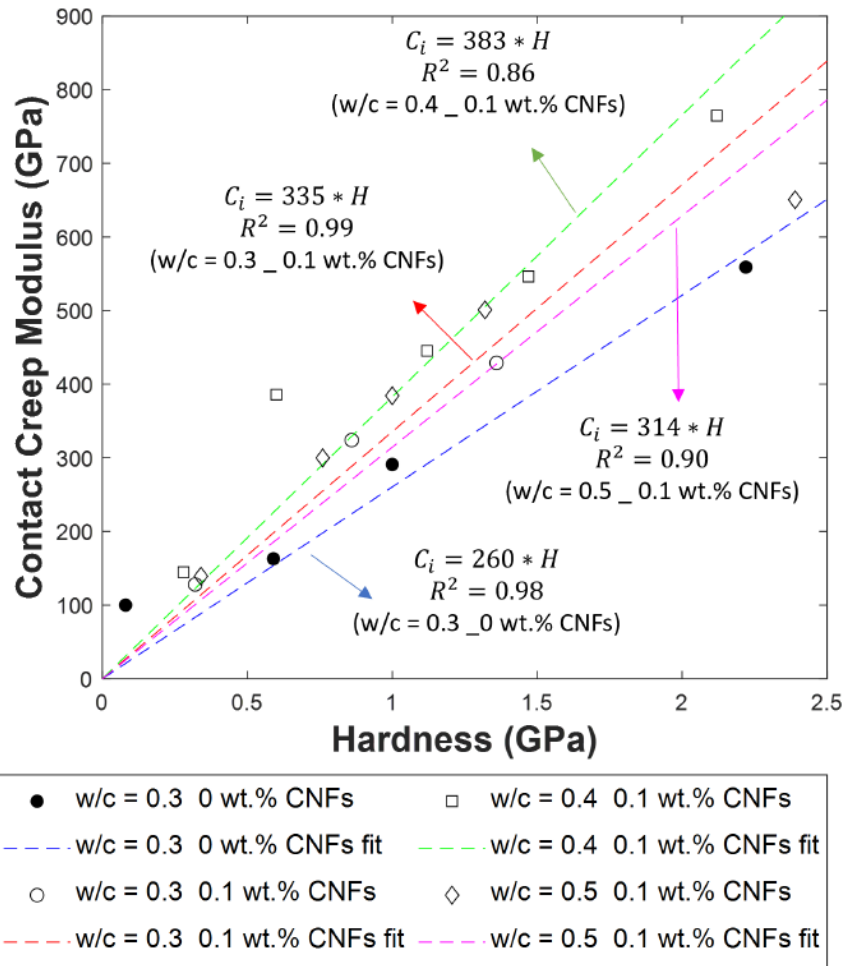


Figure 6: Relationship between contact creep modulus and hardness for varying w/c cement pastes with and without CNF. Relationship is modeled as linear with CNF-reinforced samples exhibiting higher contact creep moduli at similar hardness values compared to unreinforced samples.

Conclusions

Although interrupted and altered by COVID and other related factors, the present study has expanded the body of knowledge of nanomodification of cementitious composites, particularly related to dispersion of nanomaterials, and nano/microscale creep behavior. The specific findings of this study include:

1. Individual dispersed CNF fibers can be imaged via AFM or SEM following a drop test to isolate fibers.
2. Significant fiber breakage is occurring during the mechanical agitation typically employed to disperse CNF.
3. Nanoindentation can be used to measure elastic modulus, hardness, and contact creep modulus, for multiple hydrate phases in cement paste.

4. The contact creep modulus is higher in CNF-modified cement pastes, which indicates that lower creep strains should be expected.
5. The increased contact creep modulus is partially explained by an increased hardness in the C-S-H regions of nanomodified cement pastes (likely due to physical reinforcement), but there is also an inherent increase in the rate of contact creep modulus increase with hardness, which is likely tied to chemical or structural changes to the C-S-H in the presence of CNF.

References

- [1] Makar, J.M. and Beaudoin, J.J., 2004. Carbon nanotubes and their application in the construction industry. *Special Publication-Royal Society Of Chemistry*, 292, pp.331-342.
- [2] Parveen, S., Rana, S. and Fanguero, R., 2013. A review on nanomaterial dispersion, microstructure, and mechanical properties of carbon nanotube and nanofiber reinforced cementitious composites. *Journal of Nanomaterials*, 2013, p.80.
- [3] Metaxa, Z.S., Konsta-Gdoutos, M.S. and Shah, S.P., 2009. Carbon nanotubes reinforced concrete. *Special Publication*, 267, pp.11-20.
- [4] Shah, S.P. and Konsta-Gdoutos, M.S., 2017. Uncoupling modulus of elasticity and strength. *Concrete International*, 39(11), pp.37-42.
- [5] Zhu, X., Gao, Y., Dai, Z., Corr, D.J. and Shah, S.P., 2018. Effect of interfacial transition zone on the Young's modulus of carbon nanofiber reinforced cement concrete. *Cement and Concrete Research*, 107, pp.49-63.
- [6] Gao, Y., Zhu, X., Corr, D.J., Konsta-Gdoutos, M.S. and Shah, S.P., 2019. Characterization of the interfacial transition zone of CNF-Reinforced cementitious composites. *Cement and Concrete Composites*, 99, pp.130-139.
- [7] Sobolkina, A., Mechtcherine, V., Khavrus, V., Maier, D., Mende, M., Ritschel, M. and Leonhardt, A., 2012. Dispersion of carbon nanotubes and its influence on the mechanical properties of the cement matrix. *Cement and Concrete Composites*, 34(10), pp.1104-1113.
- [8] Metaxa, Z.S., Seo, J.W.T., Konsta-Gdoutos, M.S., Hersam, M.C. and Shah, S.P., 2012. Highly concentrated carbon nanotube admixture for nano-fiber reinforced cementitious materials. *Cement and Concrete Composites*, 34(5), pp.612-617.
- [9] Konsta-Gdoutos, M.S., Metaxa, Z.S. and Shah, S.P., 2010. Highly dispersed carbon nanotube reinforced cement-based materials. *Cement and Concrete Research*, 40(7), pp.1052-1059.

- [10] Gao, Y., Corr, D.J., Konsta-Gdoutos, M.S. and Shah, S.P., 2018. Effect of Carbon Nanofibers on Autogenous Shrinkage and Shrinkage Cracking of Cementitious Nanocomposites. *ACI Materials Journal*, 115(4), pp.615-622.
- [11] Mendu K., Guiney L.M, Hersam M.C., Shah S.P. and Corr D.J., 2023. Characterization and scalability of carbo nanofiber dispersions in aqueous solutions for cementitious nanocomposites. *Cement and Concrete Composites*, under review.
- [12] Mendu K., 2022. Multiscale characterization of nanomodified cementitious composites. Ph.D. dissertation, Civil and Environmental Engineering, Northwestern University.
- [13] Marerro-Rosa R., Corr D.J., and Shah S.P., 2023. Characterization of Contact Creep Behavior in Carbon Nanoreinforced Cementitious Composites, in preparation
- [14] Marerro-Rosa R., 2022. Studying carbon nanoreinforced cementitious composite fundamental properties through contact mechanics. Ph.D. dissertation, Civil and Environmental Engineering, Northwestern University.